Inversion of azimuthal seismic amplitude differences for tilted fracture weaknesses

Huaizhen Chen* and Kristopher Innanen

*huaizhen.chen@ucalgary.ca

Abstract

We first express stiffness matrix of tilted transversely isotropic (TTI) media in terms of the normal and tangential fracture weaknesses. Using perturbations in stiffness parameters for the case of an interface separating an isotropic medium and a TTI medium, we derive a linearized P-to-P reflection coefficient as a function of fracture weaknesses, in which titled fracture weaknesses involving effects of tilt angle and fracture weaknesses emerge. Following a Bayesian framework, we propose an inversion approach to use amplitude differences between seismic data along two azimuths to estimate the tangential fracture weakness and tilted normal and tangential fracture weaknesses based on the derived and simplified reflection coefficient. Synthetic tests confirm that the unknown parameter vector involving the tangential fracture weakness and tilted fracture weaknesses is estimated stably and reliably in the case of seismic data containing a moderate Gaussian noise. The inversion approach is also applied to a field data set acquired from a fractured carbonate reservoir, from which reasonable results of tilted fracture weaknesses are obtained. We conclude that the proposed inversion approach may provide additional proofs for fracture characterization, and it also make the estimation of tilt angle from observed seismic data for fractured reservoirs be available.

Theory and Method

1. Stiffness matrix related to fracture weaknesses

The stiffness matrix of a TTI medium, $\mathbf{C}_{\mathrm{TTI}}$, is expressed using the stiffness matrix of a corresponding VTI medium, $\mathbf{C}_{\mathrm{VTI}}$, which is given by (Auld, 1990)

$$\mathbf{C}_{\mathrm{TTI}} = \mathbf{M}_{\nu}\mathbf{C}_{\mathrm{VTI}}\mathbf{M}_{\nu}^{T}, \tag{1}$$

where $\mathbf{M}_{\nu}^{T}$ is the transpose of $\mathbf{M}_{\nu}$, ν denotes the tilt angle. In the case of $\nu = 90^{\circ}$, the TTI medium becomes the HTI medium, and in the case of $\nu = 0^{\circ}$, the TTI medium becomes the VTI medium.

In the linear slip model, the stiffness matrix of the HTI medium is given by (Schoenberg and Sayers, 1995)

$$\mathbf{C}_{\mathrm{HTI}} = \begin{bmatrix} M(1-\delta_N) & \lambda(1-\delta_N) & \lambda(1-\delta_N) & 0 & 0 & 0 \\ \lambda(1-\delta_N) & M\left(1-\chi^2\delta_N\right) & \lambda(1-\chi\delta_N) & 0 & 0 & 0 \\ \lambda(1-\delta_N) & \lambda(1-\chi\delta_N) & M\left(1-\chi^2\delta_N\right) & 0 & 0 & 0 \\ 0 & 0 & 0 & \mu & 0 & 0 \\ 0 & 0 & 0 & 0 & \mu(1-\delta_T) & 0 \\ 0 & 0 & 0 & 0 & 0 & \mu(1-\delta_T) \end{bmatrix}, \tag{2}$$

where $M = \lambda + 2\mu$, λ and μ are Lamé constants of the homogeneous isotropic host rock, $\chi = \lambda/M$, and δ_N and δ_T are the normal and tangential fracture weaknesses.

Letting the tilt angle ν be 90° and $\mathbf{C}_{\mathrm{TTI}}$ be equal to $\mathbf{C}_{\mathrm{HTI}}$, we use equation 1 to obtain the expression of the stiffness matrix of the corresponding VTI medium

$$\mathbf{C}_{\mathrm{VTI}} = \left(\mathbf{M}_{\nu=90^{\circ}}\right)^{-1}\mathbf{C}_{\mathrm{HTI}}\left(\mathbf{M}_{\nu=90^{\circ}}^{T}\right)^{-1}, \tag{3}$$

where $\left(\mathbf{M}_{\nu=90^{\circ}}\right)^{-1}$ and $\left(\mathbf{M}_{\nu=90^{\circ}}^{T}\right)^{-1}$ are the inverse matrices of $\mathbf{M}_{\nu=90^{\circ}}$ and $\mathbf{M}_{\nu=90^{\circ}}^{T}$, respectively.

Combining equations 1-3, we obtain the stiffness parameters of the TTI medium in terms of fracture weaknesses.

2. Derivation of P-to-P reflection coefficient for TTI media

Using the derived stiffness parameters, we first express perturbations in stiffness parameters for the case of one interface separating an isotropic layer and a TTI layer. The derived linearized reflection coefficient for the interface separating an isotropic layer and a TTI layer is given by

$$\begin{aligned} R_{\mathrm{PP}}(\theta,\phi) = {} & 0.5\sec^2\theta R_M - \left[4\sin^2\theta + 2\left(\cos^2\nu - \cos^4\nu\right)\right] R_{\mu} \\ & + \left(1 - 0.5\sec^2\theta\right) R_{\rho} - \begin{bmatrix} 1/4\sec^2\theta(1-2g)^2 + g(1-2g)\tan^2\theta\cos^2\phi \\ +g^2\cos^2\theta\cos^4\nu - g(1-2g)\tan^2\theta\cos^2\phi\cos^2\nu \\ g(1-2g)\cos^2\nu + g^2\sin^2\theta\tan^2\theta\cos^4\phi\sin^4\nu \end{bmatrix}\delta_N \\ & + g\begin{bmatrix} 2\sin^2\theta\cos^2\phi - \tan^2\theta\cos^2\phi \\ 2\sin^2\theta\cos^2\phi\cos^4\nu + \sin^2\theta\tan^2\theta\cos^4\phi\sin^4\nu \\ -4\sin^2\theta\cos^2\phi\cos^2\nu + \tan^2\theta\cos^2\phi\cos^2\nu + \sin^2\theta\cos^2\nu \end{bmatrix}\delta_T, \end{aligned} \tag{4}$$

Theory and Method

where $g = \mu/M$, and R_M, R_{μ} and R_{ρ} are reflectivities of P- and S-wave moduli and density, respectively. Based on the reflection coefficient, we express the difference between the reflection coefficients at two azimuthal angles (ϕ_1 and ϕ_2)

$$\begin{aligned} \Delta R_{\mathrm{PP}} = {} & R_{\mathrm{PP}}(\theta,\phi_2) - R_{\mathrm{PP}}(\theta,\phi_1) = -g\sin^2\theta\left(\cos 2\phi_2 - \cos 2\phi_1\right)\delta_T \\ & - g(1-2g)\tan^2\theta\left(\cos^2\phi_2 - \cos^2\phi_1\right)\delta_{\nu N} \\ & + g(4\sin^2\theta - \tan^2\theta)(\cos^2\phi_2 - \cos^2\phi_1)\delta_{\nu T}, \end{aligned} \tag{5}$$

where $\delta_{\nu\mu} = \sin^2\nu\Delta\mu/\mu$, $\delta_{\nu N} = \sin^2\nu\delta_N$ and $\delta_{\nu T} = \sin^2\nu\delta_T$ are named tilted S-wave modulus reflectivity and fracture weaknesses. Under the assumption that the P-wave incidence angle is less than 30°, we neglect the term proportional to $\sin^2\theta\tan^2\theta$, and in the case that fractures have a high tilt angle, we neglect the term proportional to $\cos^4\nu$.

3.Azimuthal seismic inversion for tangential fracture weaknesses and tilted fracture weaknesses

We next present an approach of using azimuthal seismic amplitude differences to estimate unknown parameters (i.e. δ_T, $\delta_{\nu N}$ and $\delta_{\nu T}$). In the case of n reflection interface and m incidence angle, the seismic amplitude difference is generated by

$$\mathbf{d} = \mathbf{G}\mathbf{x}, \tag{6}$$

where

$$\mathbf{d} = \begin{bmatrix} \mathbf{W}R_{\mathrm{PP}}(\theta_1,\phi_2) - \mathbf{W}R_{\mathrm{PP}}(\theta_1,\phi_1) \\ \vdots \\ \mathbf{W}R_{\mathrm{PP}}(\theta_m,\phi_2) - \mathbf{W}R_{\mathrm{PP}}(\theta_m,\phi_1) \end{bmatrix}_{mn\times 1}, \mathbf{W} = \begin{bmatrix} w_1 & 0 & \dots & 0 \\ w_2 & w_1 & \ddots & \vdots \\ \vdots & \vdots & \ddots & 0 \\ w_n & w_{n-1} & \dots & w_1 \end{bmatrix}_{n\times n},$$

$$\mathbf{x} = \begin{bmatrix} R_{\delta_T} \\ R_{\delta_{\nu N}} \\ R_{\delta_{\nu T}} \end{bmatrix}_{3n\times 1}, \mathbf{G} = \begin{bmatrix} \mathbf{A}(\theta_1) & \mathbf{B}(\theta_1) & \mathbf{C}(\theta_1) \\ \vdots & \vdots & \vdots \\ \mathbf{A}(\theta_m) & \mathbf{B}(\theta_m) & \mathbf{C}(\theta_m) \end{bmatrix}_{mn\times 3n}, \tag{7}$$

and where $w_1, \dots, w_n$ are elements of wavelet extracted from input seismic data.

We next propose an approach to constrain the inversion problem using probabilistic constraints. Following a Bayesian framework, the posterior Probability Distribution function (PDF) is given by (Buland and Omre, 2003)

$$P(\mathbf{x}|\mathbf{d}) \propto P(\mathbf{d}|\mathbf{x})\,P(\mathbf{x}), \tag{8}$$

where $P(\mathbf{x}|\mathbf{d})$ is the posterior PDF, $P(\mathbf{d}|\mathbf{x})$ is the likelihood function, and $P(\mathbf{x})$ is the prior constraint PDF. Under the assumptions of Gaussian random noise/error embedding in the input seismic data and the priori constraint following the Cauchy distribution, we express the posterior PDF as

$$P(\mathbf{x}|\mathbf{d}) \propto \mathcal{P}\exp\left[J(\mathbf{x})\right], \tag{9}$$

where

$$J(\mathbf{x}) = (\mathbf{d} - \mathbf{G}\mathbf{x})^T(\mathbf{d} - \mathbf{G}\mathbf{x})/2\sigma_{\mathrm{e}}^2 + \sum_{i=1}^{3n}\ln\left(1 + x_i^2/\sigma_{\mathbf{x}}^2\right). \tag{10}$$

Differentiating $J(\mathbf{x})$ with respect to $\mathbf{x}$, and letting the resulting expression be zero yields

$$\left(\mathbf{G}^T\mathbf{G} + \frac{2\sigma_{\mathrm{e}}^2}{\sigma_{\mathbf{x}}^2 + x_i^2}\right)\mathbf{x} = \mathbf{G}^T\mathbf{d}. \tag{11}$$

The iterative re-weighted least squares(IRLS) algorithm is employed to solve the inversion problem.

Numerical modeling

We first use a well log model to generate synthetic seismic amplitude differences, and then we implement the inversion for the tangential fracture weaknesses and tilted fracture weaknesses to verify the stability and robustness of the proposed approach. In Figure 1a, we show curves of P- and S-wave velocities (V_{P} and V_{S}), density ρ, and fracture density e, and in Figure 1b, we compute the tangential fracture weakness and tilted fracture weaknesses given different values of tilt angle ν.

Numerical modeling

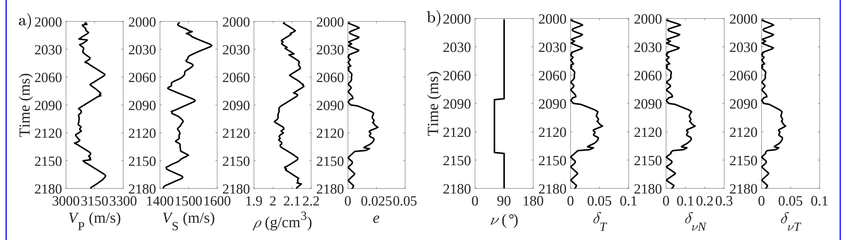

Fig 1. A well log model.

Comparisons between true and inversion values of tangential fracture weakness and tilted fracture weaknesses are plotted in Figure 2.

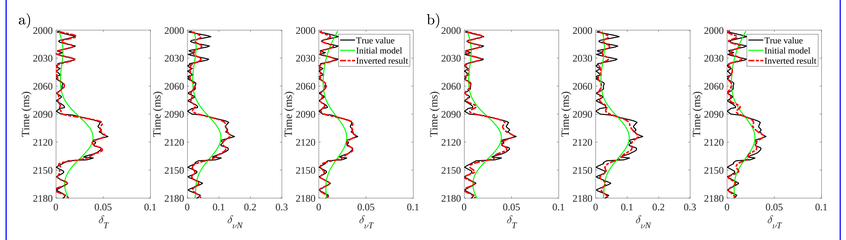

Fig 2. Comparisons between true values and inversion results. (a) No noise and (b) SNR=5.

We proceed to applying the proposed approach to a real data set to further confirm its feasibility. The data have been sorted to common azimuth gathers, and they are also transformed from offset to the incidence angle for each azimuth sector. In Figure 3, we plot stacked CDP seismic profiles along azimuths ϕ_1 and ϕ_2 and the differences between stacked seismic profiles. The ellipse in the figure indicates the location of the fractured reservoir. Inversion results are plotted in Figure 4.

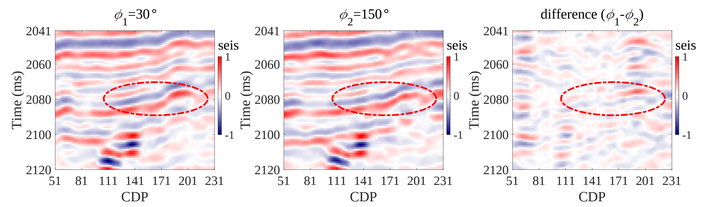

Fig 3. Stacked CDP seismic profiles and the differences between azimuthal stacked seismic data.

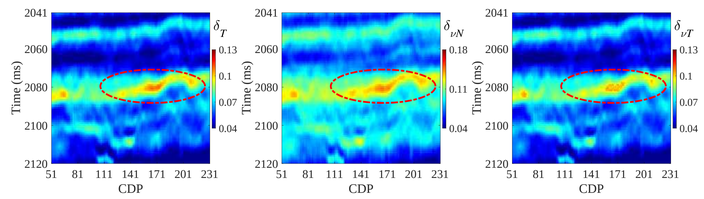

Fig 4. Inversion results of tilted fracture weaknesses.

Conclusions

We derive a linearized reflection coefficient in terms of tilted fracture weaknesses, and we propose an inversion approach to employ amplitude differences to estimate tilted fracture weaknesses. Tests on synthetic and real seismic data confirm the stability and reliability of the proposed inversion approach.

Acknowledgement

The industrial sponsors of CREWES are thanked for their supports. We gratefully acknowledge support from NSERC through the grant CRDPJ 461179-13. This research was undertaken thanks in part to funding from CFREF project. Sinopec is thanked for data use agreement.